

Benchtop ^{129}Xe optical polarizer for NMR applications

D. Radnatarov, S. Kobtsev, V. Andryushkov.

Division of Laser Physics and Innovative Technologies, Novosibirsk State University, Pirogova str.,
2, Novosibirsk, Russia 630090

ABSTRACT

The present work proposes and studies a table-top ^{129}Xe spin-exchange optical pumping polariser implementing a novel concept of interchangeable small-volume gas cells. The identified effect of relatively broadband medium absorption enabled efficient polarisation of ^{129}Xe nuclear spins within volumes of tens of millilitres by the radiation from commercial diode lasers with output powers of several W and the output line width of about 1 nm. Details of the developed device are presented, and its application in various industrial fields are discussed.

Keywords: xenon hyperpolarisation, SEOP, spin-exchange, NMR, rubidium, optical dense.

1. INTRODUCTION

Hyper-polarised (HP) noble gases are today considered as promising contrast media¹ in nuclear magnetic resonance (NMR) spectroscopy and tomography in such applications as diagnosis of human pulmonary² and brain³ diseases, material science, studies in ultra-weak fields⁴, and so forth. Noble gases with nuclear spin $I=1/2$, most sensitive to the surrounding substances, include helium-3 and xenon-129, but owing to ready availability and comparatively low cost, it was HP xenon-129 that gained the broadest application⁵. Among the diversity of the existing methods for gas hyper-polarisation (brute force polarisation, BFP⁶; metastability exchange optical pumping (MEOP)⁷; dynamic nuclear polarisation (DNP)⁸; parahydrogen-induced polarisation (PHIP)⁹ and others), it is the spin-exchange optical pumping (SEOP)¹⁰, in which circularly polarised radiation is absorbed by an alkali metal vapour, that became most widely used. In this process, electron spin polarisation in the alkali metal atoms is created and then—as a result of spin exchanges after collisions with xenon-129 atoms—transferred to their nuclei, thus producing a polarised noble gas population.

In many aspects, the progress in spin-exchange polarisation of noble gases is due to the prospect of clinical applications of HP xenon, which set the requirement for production rate at the level of 10–1,000 litres a day, something possible with a powerful (> 100 W) laser radiation having the line width within 0.1 nm¹¹. The demand for high-throughput systems spurred introduction of the first commercial systems for production of HP xenon at the rate of ~ 1 l/hour^{12–15}.

Alongside, however, there is an enormous range of problems related to applied NMR spectroscopy, which do not require large volumes of polarised gas for making an individual measurement, and in these cases a few millilitres of gas would be enough to fill a test tube^{16,17}. Therefore, many research groups relying on NMR spectroscopy in their activities are forced to develop and maintain their own relatively compact polarisers on the basis of available less powerful laser sources^{18–21}. Among the most wide-spread types of lasers used in those polarisers are narrow-band Ti:Sa lasers (whose output power usually does not exceed 1 W^{22,23}) or laser diodes with a considerably broader output radiation line and, consequently, higher output power (exceeding 10–100 W^{24,25}). In these cases, the polarisation degree of tens per cent can only be achieved at xenon concentrations within several per cent of the gas mix²⁶, which may not always be sufficient for generation of a satisfactory NMR signal. The other problem is the requirement of periodical maintenance of the polariser cells, which consists in removal from the cell walls of oxidation products and deposition into the cell of a new dose of the alkali metal. This kind of procedures—because of extremely high chemical activity of rubidium—require special equipment and certain level of qualification of the personnel.

In this connection, it becomes an important task to develop a low-cost table-top polariser on the basis of commercially available components that would allow production of small volumes of polarised gas sufficient for one or two NMR measurements, and in which an inexpensive disposable alkali metal cell could be used that could be replaced after few dozens of production cycles.

The present work proposes and studies a table-top ^{129}Xe spin-exchange optical pumping polariser implementing a novel concept of interchangeable small-volume gas cells. This simple device is based on an original concept of hyperpolarisation of small gas quantities sufficient for many purposes. The final degree of ^{129}Xe nuclear spin polarisation exceeds that of thermal equilibrium by 3–4 orders of magnitude. We report on study of the identified effect of comparatively broadband radiation absorption, which makes it possible to pump Rb vapour with radiation whose line width by more than an order of magnitude exceeds the width of ordinary Doppler absorption contour in Rb. The effective spectral absorption width grows as the cell length and metal vapour concentration increase. The identified effect of relatively broadband radiation requires certain parameters of the absorption cell (such as that the cell length should be larger than its transverse dimension and that the buffer gas should have relatively high pressure).

This work presents the design of the absorption cell with optimised radiation absorption length (~100 mm), an analysis of the optimal conditions for polarisation and a concept of a tabletop system for ^{129}Xe hyperpolarisation.

2. POLARISER PROTOTYPE

2.1 Polarizer

For polarisation of xenon via spin-exchange optical pumping, the following basic components are needed: circularly polarised optical radiation at the wavelength corresponding to the absorption line of the chosen alkali metal (rubidium in our case), optical cell containing alkali metal vapour and xenon, magnetic field parallel to the optical axis. Under the action of circularly polarised optical radiation in the presence of magnetic field, rubidium electrons acquire spin polarisation, which is then transferred to xenon nuclei by collisions.

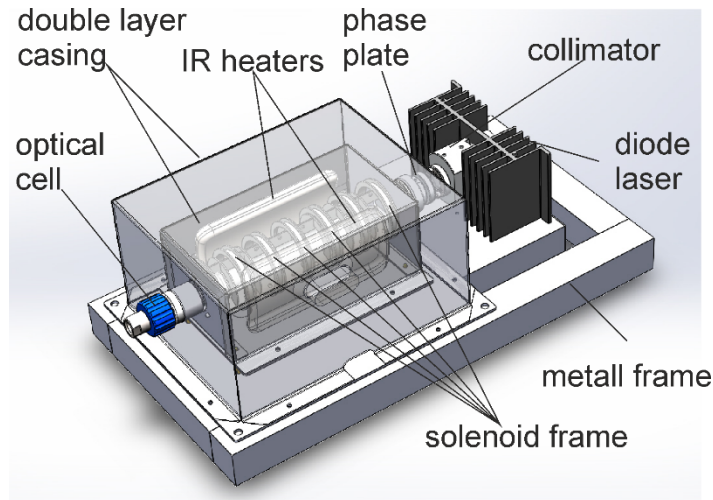


Figure 1. 3D view of the optical train of the table-top polariser.

A prototype diagram of a table-top polariser is presented in Fig. 1. Linearly polarised radiation from a laser diode emitting at ~795 nm is collimated with a lens, then passes through a quarter-wave plate, thus acquiring circular polarisation, and is further guided into an optical cell about 10-cm long (a detailed description of the cell design will be found in the following subsection). At the end of the cell, there is a metal mirror bending the radiation emerging from the cell by 90°. That radiation is registered with a photo-detector

In order to create a magnetic field inside the optical cell, a system of six 5-mm wide solenoids uniformly distributed along the cell was used, the field strength at the cell axis reaching about 5 mT at the current of 2 A. For heating the cell and maintaining a high density of rubidium vapour, IR heaters were used with the total power of 1 kW. The heating time to 100°C for this cell was about 2 minutes. The heated area was insulated with a double-layer cover having an opening for quick installation and removal of the cell, and also with an opening at the bottom of the cover for the exiting radiation. The

entire set-up was affixed to an extruded aluminium frame, under which were placed power supplies, laser diode and IR heater drivers. Also, a control panel was installed with controls and indicators for adjustment of the laser diode injection current, cell temperature, turning on the solenoid current, and measurement of the power of radiation exiting from the cell (see Fig. 2).

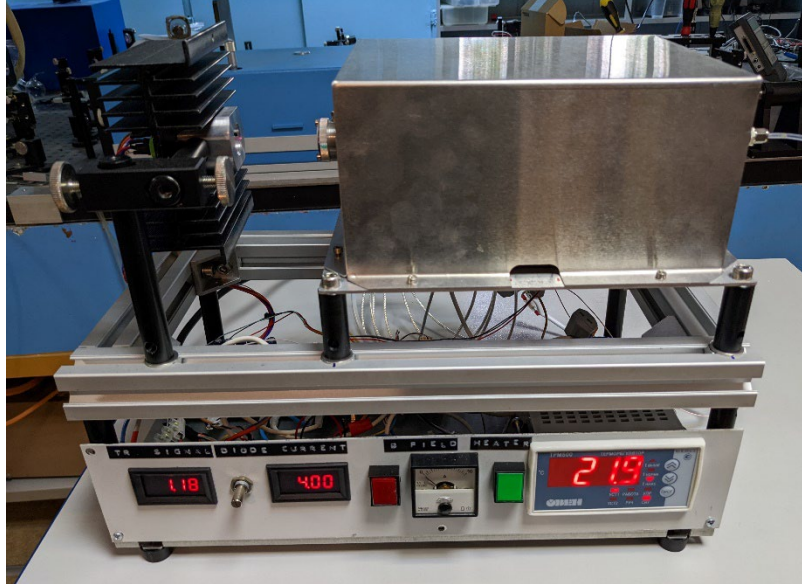


Figure 2. Photograph of the prototype table-top xenon polariser.

The dimensions of this installation were 40x30x20 cm (LxHxW) and the weight about 3 kg.

In order to achieve a high polarisation degree of xenon nuclear spins, it is necessary to ensure powerful optical pumping of the alkali metal vapour, which, in its turn, depends upon the number of photons absorbed from the pump radiation. When the used radiation has a line width exceeding that of the medium absorption line, it is possible to achieve stronger absorption by elongation of the cell and increasing the rubidium atom concentration. In this case, the absorption line width is determined by the properties of alkali metal atoms, but the absorbed radiation line width is broadened (mathematical difference between the radiation spectrum prior to and after the cell). In low-absorbance medium, both these spectra are essentially the same and the absorption line width is equal to the width of the absorbed radiation spectrum. However, in highly absorbing medium where pumping depletion occurs (i.e. significant decrease of the optical intensity in the centre of the absorption line), the absorbed radiation spectrum may be substantially, by a few orders of magnitude, broadened. The medium absorption coefficient, in this case will be determined not only by the ratio of the atomic absorption line width and the pumping radiation spectral width, but also by the optical absorbance of the medium

In our prototype, we used a commercial model of 4-W diode laser with a typical output line width of 2 nm. Fig. 2a shows the radiation spectra at the exit of the cell at different cell temperatures. The graph demonstrates that at 60°C—when rubidium atom concentration is comparatively low—the dip width (and that of the peak in the absorbed radiation spectrum, see Fig. 3b) is only 0.1 nm, corresponding to the impact-broadened absorption line width at the gas mix pressure of 4.5 atm. The absorption in this case was 4%. At higher temperature of 100 °C, the dip width (and that of the peak in the absorbed radiation spectrum) grew to 1.3 nm, the absorption growing to 17%. Subsequent increase in the cell temperature to 150 °C may boost absorption to over 50%. An optimal temperature exists, at which the maximal polarisation of xenon nuclei is achieved. At this temperature, a balance is struck between growing number of absorbed photons and pump depletion, which causes polarisation degree to drop progressively from the input end of the cell to the output.

Our preliminary experiments have shown that the optimal cell temperature lies within the 90–100 °C range, the absorption measuring around 10–17%. For estimation of the xenon nuclear polarisation degree, we used the approach earlier presented in works^{27,28} that is based on measurement of the transmitted radiation with and without magnetic field in cold and hot cell. This method produces the estimate of over 40% degree of xenon nuclear polarisation. Although it is more suitable for the case of low optical absorbance and in our case clearly gives too high results, it may probably be used for qualitative measurements during preliminary optimisation of the polarisation conditions

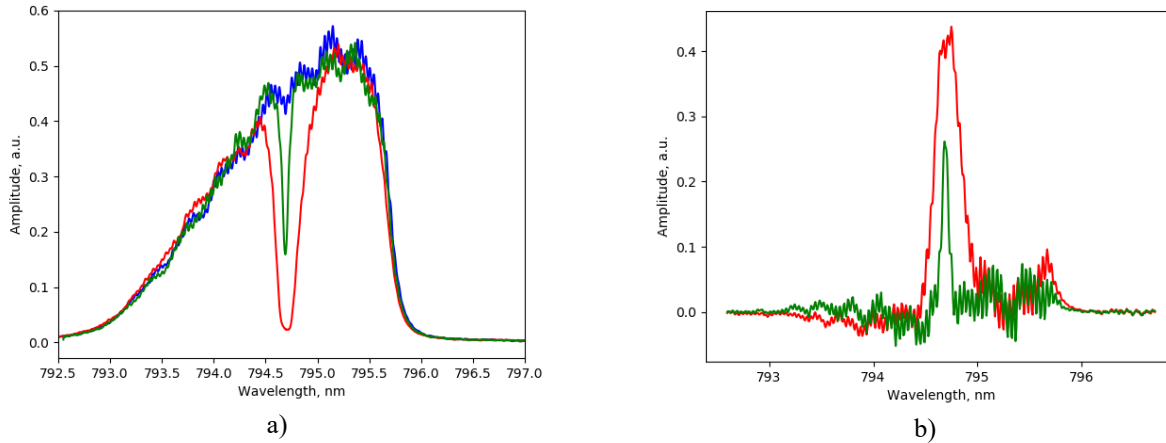


Figure 3. a) Radiation spectrum at the exit of the cell at different cell temperatures: blue curve –20°C, green curve – 60°C, red curve – 100°C. b) Absorbed radiation spectrum (mathematical difference between the spectra before and after the cell) at different cell temperatures: green curve – 60°C, red curve –100°C.

2.2 Cell

The optical cell was made from a high-pressure (up to 6 atm) borosilicate test tube with thick walls for chemical synthesis. Since these tubes are mass-manufactured, they exhibit minimal geometrical variations from one sample to another. This makes it possible to avoid readjustment of the optical system for each particular cell, a procedure sometimes necessary when manually glass-blown cells are used.

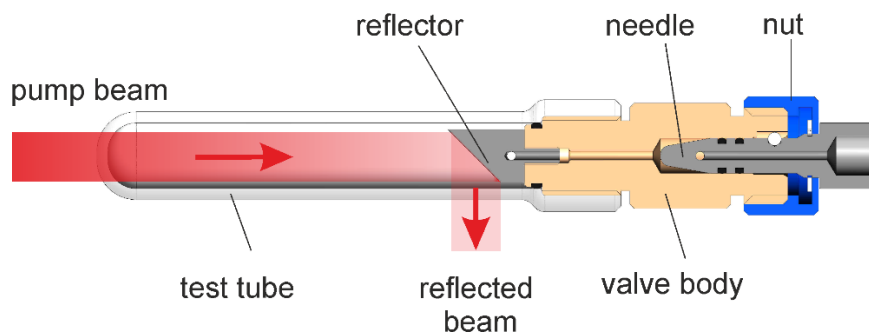


Figure 4. Optical cell diagram.

A picture of the cell is given in Fig. 2. The test tube had the volume of 10 ml, its outer diameter being 20 mm, wall thickness 3 mm, and length, 100 mm. The tube cap was replaced by a made in-house needle valve. The valve base was made of PTFE with a titanium alloy needle. As the valve knob is rotated, the needle moves along its axis, shifting out of a fluoroplastic seat, thus allowing gas flow in or out of the tube. Thanks to this axially symmetric design, the gas supply tubing exits from the magnetic field created by the polariser solenoids along their axis, thus reducing the risk of passing through a zero-field space, which would lead to immediate depolarisation of xenon. Inside the cell, a polished titanium reflector is installed for bending the pumping radiation by 90°. The choice of materials for the valve is dictated by extreme chemical activity of rubidium, as well as by the need to avoid any ferrimagnetic parts, which could create local magnetic fields and thus depolarise xenon atoms.

In the first batch, 4 copies of the optical cell were fabricated (see Fig. 4). Each of them was tested for air-tightness by evacuation down to $1 \cdot 10^{-2}$ torr (the residual pressure of the vacuum station). Opening or closing of the valve upon reaching the lowest possible pressure did not produce any change of pressure in the vacuum system. Approximately 150 mg of rubidium was deposited into each cell, the procedure being performed inside a glove box with an inert atmosphere.



Figure 5. Photograph of the first four cells after rubidium deposition.

Additionally, the gas leakage rate from the cells was measured at high internal pressure. For this, the cells already containing rubidium were filled with the gas mix at 5 atm and stored away at normal ambient conditions and temperature of 22–25 °C. Measurements conducted after 73 days have shown that the internal pressure drop in the cells was within 2.5%, which is comparable to the precision of the available pressure gauge. After this period, the rubidium droplets kept their metallic shine, indicating that there was practically no ingress of oxygen into the cell. These measurements confirm the possibility of long-term storage of cells charged with rubidium

3. NMR EXPERIMENT

From the practical viewpoint, we were interested in the possibility of using a table-top polariser in conjunction with an NMR spectrometer in order to develop the procedure of filling the NMR spectrometer cell and to measure the resulting polarisation degree of xenon. For this, the polariser prototype with a set of rubidium cells was temporarily moved into a laboratory where an NMR spectrometer with the magnetic field strength of 9.4 T was installed. The schematic diagram of the experiment on practical use of the developed polariser is presented in Fig. 6. The cells of the polariser and the NMR spectrometer were connected with a thin (internal diameter below 2 mm) fluoroplastic tube through a three-way valve also connected to a vacuum pump. Prior to the experiment, the vacuum pump removed air from the tubing and then was cut off. The valve in the polariser cell was opened and the gas mix filled the NMR spectrometer cell at the resulting pressure

of ~1 atm. In the course of this experiment, it was found out that proper evacuation of the gas tubing is a critical step that may take several hours if PTFE tubing is used. As a result of multiple experiments on measurement of the xenon nuclear polarisation state, the best reading was 1.34%, which exceeds by a factor of 1680 the equilibrium polarisation of xenon in the field of the NMR spectrometer. The results were calibrated against the earlier recorded NMR spectrum of xenon, which was measured after filling the spectrometer cell with pure xenon at the pressure of 4 atm. Before these measurements, xenon was thermalised during 18 hours.

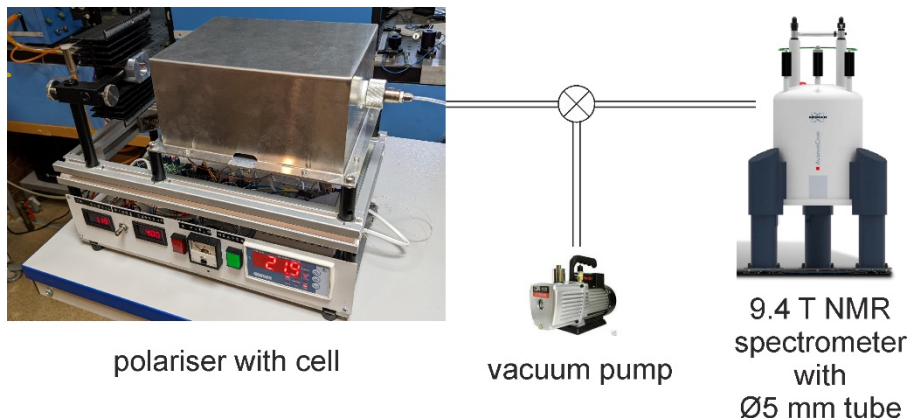


Figure 6. Layout of the experiment on NMR spectroscopy of polarised xenon.

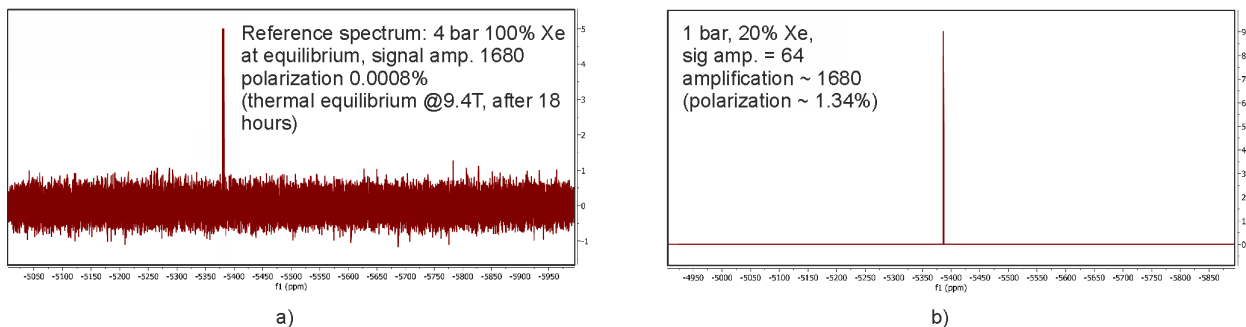


Figure 7. NMR spectra of xenon: a) equilibrium polarisation, b) polarisation after the table-top polariser.

4. CONCLUSION

In this work, a prototype of a table-top xenon polariser was demonstrated, which was based on a diode laser with the output power of 4 W and radiation line width of 2 nm. Also demonstrated was an original design of the optical cell based on a type of mass-produced test tubes. The achieved level of xenon polarisation was 1.34%, which is sufficient for many NMR measurements, including characterisation of various porous materials.

ACKNOWLEDGEMENTS

The work was supported by the Russian Science Foundation (grant No. 22-22-00264). The work of S. Kobtsev (problem definition, component testing, technical designs of the device) received support of the Ministry of Science and Higher Education of the Russian Federation (FSUS-2020-0036). We would like to express our appreciation to the Zhukov I. and Pokochueva E. for the organization and conduct of the NMR-spectroscopy experiments.

REFERENCES

- [1] Jiménez-Martínez, R., Kennedy, D. J., Rosenbluh, M., Donley, E. A., Knappe, S., Seltzer, S. J., Ring, H. L., Bajaj, V. S., Kitching, J., "Optical hyperpolarization and NMR detection of ^{129}Xe on a microfluidic chip," *Nat. Commun.* **5** (May) (2014).
- [2] Mugler, J. P., Altes, T. A., "Hyperpolarized ^{129}Xe MRI of the human lung," *J. Magn. Reson. Imaging* **37** (2), 313–331 (2013).
- [3] Swanson, S. D., Rosen, M. S., Agranoff, B. W., Coulter, K. P., Welsh, R. C., Chupp, T. E., "Brain MRI with laser-polarized ^{129}Xe ," *Magn. Reson. Med.* **38** (5), 695–698 (1997).
- [4] Tayler, M. C. D., Theis, T., Sjolander, T. F., Blanchard, J. W., Kentner, A., Pustelny, S., Pines, A., Budker, D., "Invited review article: Instrumentation for nuclear magnetic resonance in zero and ultralow magnetic field," *Rev. Sci. Instrum.* **88** (9), 091101 (2017).
- [5] Meersmann, T., Brunner, E., eds., [Hyperpolarized Xenon-129 magnetic resonance, 4th ed.], Royal Society of Chemistry, Cambridge (2015).
- [6] Frossati, G., "Polarization of ^3He , D_2 and (eventually) ^{129}Xe using low temperatures and high magnetic fields," *J. Low Temp. Phys.* **111** (3–4), 521–532 (1998).
- [7] Colegrove, F. D., Scheerer, L. D., Walters, G. K., "Polarization of He^3 Gas by optical pumping," *Phys. Rev.* **132** (6), 2561–2572 (1963).
- [8] Maly, T., Debelouchina, G. T., Bajaj, V. S., Hu, K.-N., Joo, C.-G., Mak–Jurkauskas, M. L., Sirigiri, J. R., van der Wel, P. C. A., Herzfeld, J., Temkin, R. J., Griffin, R. G., "Dynamic nuclear polarization at high magnetic fields," *J. Chem. Phys.* **128** (5), 052211 (2008).
- [9] Bowers, C. R., Weitekamp, D. P., "Transformation of symmetrization order to nuclear-spin magnetization by chemical reaction and nuclear magnetic resonance," *Phys. Rev. Lett.* **57** (21), 2645–2648 (1986).
- [10] Walker, T. G., Happer, W., "Spin-exchange optical pumping of noble-gas nuclei," *Rev. Mod. Phys.* **69** (2), 629–642 (1997).
- [11] Whiting, N., Nikolaou, P., Eschmann, N. A., Barlow, M. J., Lammert, R., Ungar, J., Hu, W., Vaissie, L., Goodson, B. M., "Using frequency-narrowed, tunable laser diode arrays with integrated volume holographic gratings for spin-exchange optical pumping at high resonant fluxes and xenon densities," *Appl. Phys. B Lasers Opt.* **106** (4), 775–788 (2012).
- [12] Nikolaou, P., Coffey, A. M., Walkup, L. L., Gust, B. M., Whiting, N., Newton, H., Muradyan, I., Dabaghyan, M., Ranta, K., Moroz, G. D., Rosen, M. S., Patz, S., Barlow, M. J., Chekmenev, E. Y., Goodson, B. M., "XeNA: An automated 'open-source' ^{129}Xe hyperpolarizer for clinical use," *Magn. Reson. Imaging* **32** (5), 541–550 (2014).
- [13] Birchall, J. R., Nikolaou, P., Coffey, A. M., Kidd, B. E., Murphy, M., Molway, M., Bales, L. B., Goodson, B. M., Irwin, R. K., Barlow, M. J., Chekmenev, E. Y., "Batch-mode clinical-scale optical hyperpolarization of Xenon-129 using an aluminum jacket with rapid temperature ramping," *Anal. Chem.* **92** (6), 4309–4316 (2020).
- [14] "Polarean.", <http://www.polarean.com/129Xe_hyperpolarizer_9820.html>.
- [15] "XeUS Technologies LTD.", <<https://www.xeus-technologies.com/xpolarizer>>.
- [16] Weiland, E., Springuel-Huet, M.-A., Nossov, A., Gédéon, A., " ^{129}Xe NMR: review of recent insights into porous materials," *Microporous Mesoporous Mater.* **225**, 41–65 (2016).
- [17] Barskiy, D. A., Coffey, A. M., Nikolaou, P., Mikhaylov, D. M., Goodson, B. M., Branca, R. T., Lu, G. J., Shapiro, M. G., Telkki, V.-V., Zhivonitko, V. V., Koptyug, I. V., Salnikov, O. G., Kovtunov, K. V., Bukhtiyarov, V. I., Rosen, M. S., Barlow, M. J., Safavi, S., Hall, I. P., Schröder, L., et al., "NMR hyperpolarization techniques of gases," *Chem. - A Eur. J.* **23** (4), 725–751 (2017).
- [18] Zeng, Q., Bie, B., Guo, Q., Yuan, Y., Han, Q., Han, X., Chen, M., Zhang, X., Yang, Y., Liu, M., Liu, P., Deng, H., Zhou, X., "Hyperpolarized Xe NMR signal advancement by metal-organic framework entrapment in aqueous solution," *Proc. Natl. Acad. Sci. U. S. A.* **117** (30), 17558–17563 (2020).
- [19] Freeman, M., "The Efficiency limits of spin exchange optical pumping methods of ^{129}Xe hyperpolarization: implications for in vivo MRI applications," Ph.D. thesis, 1–29 (2015).
- [20] Ruset, I. C., "Hyperpolarized xenon-129 production and applications (Ph.D. thesis)" (2005).
- [21] Nelson, I. A., "Physics of practical spin-exchange optical pumping (Ph.D. thesis)" (2001).
- [22] Takeda, S., Kumagai, H., Ogawa, E., Hattori, M., "Increase of NMR/MIR signals under ultra-low B fields with hyperpolarized Xe using 1W CW single-frequency Ti:Sapphire laser," *Imaging, Manip. Anal. Biomol. Cells, Tissues XVII*(March), D. L. Farkas, J. F. Leary, and A. Tarnok, Eds., 61, SPIE (2019).

- [23] Buchta, Z., Rychnovský, J., Lazar, J., "Optical pumping of Rb by Ti:Sa laser and high-power LD," Proc. SPIE **618002** (April 2006), P. Tománek, M. Hrabovský, M. Miler, D. Senderáková, Eds., 618002-618002–618006 (2006).
- [24] Driehuys, B., Cates, G. D., Miron, E., Sauer, K., Walter, D. K., Happer, W., "High-volume production of laser-polarized ^{129}Xe ," Appl. Phys. Lett. **69** (12), 1668–1670 (1996).
- [25] Hersman, F. W., Ruset, I. C., Ketel, S., Muradian, I., Covrig, S. D., Distelbrink, J., Porter, W., Watt, D., Ketel, J., Brackett, J., Hope, A., Patz, S., "Large production system for hyperpolarized ^{129}Xe for human lung imaging studies," Acad. Radiol. **15** (6), 683–692 (2008).
- [26] Pałasz, T., Mikowska, L., Głowacz, B., Olejniczak, Z., Suchanek, M., Dohnalik, T., "Stop-flow SEOP polarizer for ^{129}Xe ," Acta Phys. Pol. A **136** (6), 1008–1017 (2019).
- [27] Nikolaou, P., Coffey, A. M., Walkup, L. L., Gust, B. M., Whiting, N., Newton, H., Barcus, S., Muradyan, I., Dabaghyan, M., Moroz, G. D., Rosen, M. S., Patz, S., Barlow, M. J., Chekmenev, E. Y., Goodson, B. M., "Near-unity nuclear polarization with an open-source ^{129}Xe hyperpolarizer for NMR and MRI," Proc. Natl. Acad. Sci. **110** (35), 14150–14155 (2013).
- [28] Nikolaou, P., Coffey, A. M., Walkup, L. L., Gust, B. M., Lapierre, C. D., Koehnemann, E., Barlow, M. J., Rosen, M. S., Goodson, B. M., Chekmenev, E. Y., "A 3D-printed high power nuclear spin polarizer," J. Am. Chem. Soc. **136** (4), 1636–1642 (2014).